Title	A mouse model of short-term, diet-induced fatty liver with abnormal cardiolipin remodeling via downregulated Tafazzin gene expression
Author(s)	Sakurai, Toshihiro; Chen, Zhen; Yamahata, Arisa et al.
Citation	Journal of the science of food and agriculture, 101(12), 4995-5001 https://doi.org/10.1002/jsfa.11144
Issue Date	2021-08-05
Doc URL	https://hdl.handle.net/2115/86499
Rights	This is the peer reviewed version of the following article: Sakurai, T., Chen, Z., Yamahata, A., Hayasaka, T., Satoh, H., Sekiguchi, H., Chiba, H., & Hui, S. P. (2021). A mouse model of short-term, diet-induced fatty liver with abnormal cardiolipin remodeling via downregulated Tafazzin gene expression. Journal of the science of food and agriculture, 101(12), 4995-5001, which has been published in final form at https://doi.org/10.1002/jsfa.11144. This article may be used for non-commercial purposes in accordance with Wiley Terms and Conditions for Use of Self-Archived Versions. This article may not be enhanced, enriched or otherwise transformed into a derivative work, without express permission from Wiley or by statutory rights under applicable legislation. Copyright notices must not be removed, obscured or modified. The article must be linked to Wiley's version of record on Wiley Online Library and any embedding, framing or otherwise making available the article or pages thereof by third parties from platforms, services and websites other than Wiley Online Library must be prohibited.
Type	journal article
File Information	20210115_MLCL_Taz_Manuscript_Resubmission_Final ver.pdf

1 **A mouse model of short-term, diet-induced fatty liver with abnormal cardiolipin**

2 **remodeling via downregulated Tafazzin gene expression**

3

4 Toshihiro Sakurai [1,*], Zhen Chen [1,*], Arisa Yamahata [1,*], Takahiro Hayasaka [1], Hiroshi Satoh [2,3],

5 Hirotaka Sekiguchi [2,4], Hitoshi Chiba [5], Shu-Ping Hui [1]

6

7 [1] Faculty of Health Sciences, Hokkaido University, Sapporo 060-0812, Japan

8 [2] Department of Food and Health Research, Life Science Institute Co. Ltd and Nissei Bio Co.

9 Ltd, Center for Food and Medical Innovation, Institute for the Promotion of Business-Regional

10 Collaboration, Hokkaido University, Sapporo, Japan

11 [3] Research and Development division, Hokkaido Research Institute, Nissei Bio Co. Ltd, Eniwa,

12 Japan

13 [4] R&D Planning and Administration Department, Life Science Institute Co., Ltd, Tokyo, Japan

14 [5] Department of Nutrition, Sapporo University of Health Sciences, Sapporo 007-0894, Japan

15

16 Correspondence: SP Hui.

17 Kita 12, Nishi 5, Kita-ku, Sapporo 060-0812, Japan.

18 E-mail: keino@hs.hokudai.ac.jp

19 * TS, ZC, and AY contributed equally.

20

21

22 Running title:

23 A short-term fatty-liver mouse model with abnormal CL remodeling

24

25 Abbreviations:

26 CL, Cardiolipin; MLCL, monolysocardiolipin; HCD, high carbohydrate diet; Taz, Tafazzin;

27 Lclat1, Lysocardiolipin acyltransferase 1; Pnpla8, Calcium-independent phospholipase A2-

28 gamma; Cls, Cardiolipin synthase; NCD, normal chow diet; ESI, electrospray ionization; PG,

29 phosphatidylglycerol.

30

31 Keywords: high-carbohydrate diet; liquid chromatography mass spectrometry; lipidomics;

32 mitochondria; monolysocardiolipin.

33

34 **Abstract**

35 **Background:** Cardiolipin (CL) helps maintain mitochondrial structure and function. Here we

36 investigated whether a high carbohydrate diet (HCD) fed to mice for a short term (5 days) can

37 modulate the CL level including that of monolysoCL (MLCL) in the liver.

38 **Results:** Total CL in the HCD group was 22% lower than that in the normal chow diet (NCD)

39 group ($P<0.05$). CL72:8 level strikingly decreased by 93% ($P<0.0001$), whereas total nascent

40 CL (CLs other than CL72:8) increased ($P<0.01$) in the HCD group. Moreover, total MLCL in

41 the HCD group increased by 2.4-fold compared with that in the NCD group ($P<0.05$). *Tafazzin*

42 expression in the HCD group was significantly downregulated compared with that in the NCD

43 group ($P<0.05$). A strong positive correlation between nascent CL and total MLCL (r $= 0.955$, P

44 <0.0001), and a negative correlation between MLCL and *Tafazzin* expression (r $= -0.593$, $P =$

45 0.0883) were observed.

46 **Conclusion:** HCD modulated fatty acid compositions of CL and MLCL via *Tafazzin* in the liver,

47 which could lead to mitochondrial dysfunction. This model may be useful for elucidating the

48 relationship between fatty liver and mitochondrial dysfunction.

49

Introduction

Cardiolipin (CL) is a crucial phospholipid containing four fatty acyl chains and is located on the inner mitochondrial membrane.[1] Nascent CL is composed of various types of fatty acyls, and monolysocardiolipin (MLCL) is formed after one of fatty acyls constituting CL is enzymatically hydrolyzed. Finally, MLCL is transformed into the mature form of CL (tetralinoleoyl-CL; CL72:8) via remodeling.[2] CL72:8 is the most abundant CL[3] and regulates mitochondrial structure and respiration,[4] biogenesis, and energy production.[5]

Abnormal CL remodeling causes the depletion of mature CL, which could contribute to the pathophysiology of several metabolic diseases.[6] Reduction in CL levels have been associated with mitochondrial dysfunction, insulin resistance,[7] non-alcoholic fatty liver,[8] and liver injury.[9,10] Furthermore, a reduction in mitochondrial activation has been reported in patients with fatty liver.[9] In our recent study, we reported that hepatosteatosis, liver dysfunction, and abnormalities in the expression of primary proteins involved in mitochondrial function and lipogenesis were observed in overeating mice fed a high carbohydrate diet (HCD) for 5 days (short term) after 2 days of fasting.[11] Although the relationship between a carbohydrate-rich diet and changes in CL composition was determined in rats fed a high amounts of sucrose for a long-term period (24 weeks),[12] similar studies on the effect of such a diet for a short term have not been performed yet.

Abnormalities in CL remodeling may be accompanied by the changes in the expression of genes involved in CL remodeling and synthesis.[1,2] Nascent CL is synthesized by cardiolipin synthase (Cls) and hydrolyzed by calcium-independent phospholipase A2-γ (Pnpla8), resulting in the formation of MLCL. MLCL is then remodeled by *Tafazzin* (*Taz*) to form mature CL. In

71   another pathway, MLCL is remodeled by lysocardiolipin acyltransferase 1 (*Lclat1*), which

72   results in the formation of inactive CL (the other CL72:8). Notably, *Taz* plays an important role

73   in the biosynthesis of mature CL (CL72:8).

74   In this study, we aimed to determine the short-term effect of HCD on a mouse model of

75   fatty liver. We investigated whether such a diet administered even for a short term modulated CL

76   and MLCL levels in the mouse liver. We also performed gene expression analysis to elucidate

77   the underlying mechanism of the abnormalities introduced in CL remodeling, and modulation of

78   CL and MLCL levels.

79 **Materials and Methods**

80 **Animal experiments**

81   All animal experimental protocols were approved by the animal care committee of

82 Hokkaido University (approval protocol number: 15-0174) as explained in a previous study.[11] In

83 this study, we used the same liver samples as those reported in a previous study. [11] Briefly, nine

84 male ddY mice (age: 7 week) were obtained from Sankyo Labo Service Corporation, Inc.

85 (Sapporo, Japan) and housed individually with *ad libitum* access to solid-type food and water.

86 Three mice comprising the control group were fed a normal chow diet (NCD) (Labo MR Stock,

87 Nosan Corporation Life-Tech Department, Yokohama, Japan) without fasting. The NCD

88 contained 3,291 kcal kg^{-1} (22.9% protein, 66.5% carbohydrate, 10.7% fat). In this study,

89 untreated mice of the same age as the HCD group were used as control mice. On the other

90 hands, six mice comprising the HCD group were fed a diet containing 380 g kg^{-1} sucrose for 5

91 days after fasting for 2 days to establish an overeating state that would lead to the development of

92 acute fatty liver.[13] The HCD, which comprised 160 g kg^{-1} milk casein, 380 g kg^{-1} sucrose, 380 g

93 kg^{-1} corn starch, 70 g kg^{-1} mineral mix, and 10 g kg^{-1} vitamin mix, was prepared from Hokudo

94 Co. Ltd. (Sapporo, Japan)(See Supplemental Table 1) and contained 3,481 kcal kg^{-1} (15.9%

95 protein, 82.8% carbohydrate, 1.3% fat). Three (control group) or six mice (experimental group)

96 were compared to minimize the number of mice possible. The mice were anesthetized and

97 sacrificed for collecting liver tissues that were stored at −80°C.

98

99 **LC/MS analysis**

100   Total lipids were extracted from the tissues by following the procedure described by

101 Hara et al.[14] Briefly, the liver tissues were treated with 3:2 (v/v) hexane/isopropanol containing

102 20 μmol/mL butylated hydroxytoluene (Wako Pure Chemical, Osaka, Japan) twice. The extracts

103 obtained were mixed and vacuum dried. The dried lipids were then dissolved in methanol (Wako

104 Pure Chemical., Osaka, Japan), centrifuged at 15,000 rpm at 4°C for 15 min to remove any

105 insoluble material, and stored at −80°C until further analysis.

106   LC/MS analysis was performed using a Shimadzu Prominence high-performance

107 liquid chromatography system equipped with an LTQ Orbitrap mass spectrometer (Thermo-

108 Fisher Scientific Inc., San Jose, CA) and an electrospray ionization (ESI) source, for which the

109 major instrumental parameters were based on our previously reported protocol.[15] The obtained

110 lipids were separated on an Atlantic T3 column (2.1 × 150 mm, 3 μm, Waters, Milford, MA). An

111 LC gradient elution was performed by using a mobile phase consisting of 5 mM aqueous

112 ammonium acetate, isopropanol, and methanol at a flow rate of 200 μL/min. For MS

113 experiments, the following parameters were kept constant for the ESI negative mode: capillary

114 voltage of −3.0 kV, capillary temperature of 330°C, sheath gas (nitrogen) flow of 50 arbitrary

115 units, and auxiliary gas (nitrogen) flow of 5 auxiliary units. High-resolution MS data were

116 obtained over a mass range of m/z 900–1650 in the Fourier transform mode with a resolving

117 power of 60,000. MS/MS data were obtained in an ion-trap mode with an isolation width of 2.0

118 Da and an activation time of 30 ms. Tandem MS data were obtained using collision induced

119 dissociation with a data-dependent mode including scans on the most intense ions, each of which

120 were in the MS2 (collision energy of −35 V) and MS3 (collision energy of −45 V) spectra.

121   For all the data, each intensity was normalized by mg of wet liver used for the analysis.

122 The raw data were processed using the workstation Xcalibur 2.2 (Thermo-Fisher Scientific Inc.),

123 including peak annotation and peak area integration. The identification of lipid molecules was

124 performed using the LIPIDMAPS database[16] and our in-house library,[15] as well as by comparing

125 the LC retention behavior and MS fragment pattern with standards. The identified lipid

126 molecular species were annotated as "class abbreviation + total carbon number in the fatty

127 chain(s) + total double bond number in the fatty chain(s)."

128   The intensity of each analyte was calculated based on the peak area that was drawn

129 using the extracted ion chromatogram with a tolerance of 5.0 ppm. For the elucidated CL types,

130 the intensity of each fatty acyl could be calculated based on the equation given below:

131

132 $$Intensity_{Fatty\ acyl} = \sum \left(Intensity_{CL\ species}^{i} \times \frac{Fatty\ acyl\ quantity_{CL\ sepcies}^{i}}{4}\right)$$

133

134 **Real-time PCR**

135   To analyze the expression of genes involved in the CL remodeling process, we

136 performed real-time PCR. Total RNA was extracted from the liver tissues (20 mg wet) using

137 PureLink® RNA Mini Kit (Thermo Fisher Scientific). The concentration and integrity of the

138 isolated RNA were determined at $OD_{260/280}$ using a NanoDrop spectrophotometer (Thermo

139 Fisher Scientific). The RNA was reverse-transcribed into cDNA using a ReverTra Ace qPCR RT

140 Master Mix (Toyobo Co., Ltd., Osaka, Japan). Real-time PCR was performed using CFX 96

141 Real-Time PCR Detection System (Bio-Rad Laboratories Inc., Hercules, CA, USA) and

142   Thunderbird® SYBR qPCR Mix (Toyobo) according to the manufacturer's instructions. The

143   sequences of primers used are given in Supplemental Table 2.[17,18] The PCR reaction was

144   performed under the following conditions: 95°C for 60 s followed by 40 cycles at 95°C for 15 s

145   and at 60°C for 30 s. The expression of all the genes was normalized to that of *Gapdh* in each

146   sample. Data are represented as the relative expression to that in the NCD group.

147

148   **Statistical analysis**

149   Student's *t*-test was performed for comparing the data between the two groups. Two-

150   way analysis of variance and the Tukey's multiple comparison test as a post-hoc test were

151   performed and are shown in Figure 1B. All the data are shown as mean ± SD. Pearson's

152   correlation coefficient was calculated to determine the relationship between total MLCL and

153   total nascent CL levels or *Taz* expression in the liver. A *P*-value of <0.05 was considered as

154   statistically significant. GraphPad Prism (version 7, GraphPad Software Inc., San Diego, CA,

155   USA) was used for performing statistical analysis.

156

157   **Results**

158   **Hepatic CL level**

159   Thirty-two types of CL were identified in the liver (Figure 1A and Supplemental Table

160   3). In the NCD group, CL72:8 was the dominant type and constituted approximately 50% of all

161   CLs. Total CL was calculated by adding the levels of all CLs detected in this study. Total CL

162   level in the HCD group was 22% lower than that in the NCD group (P <0.05) (Figure 1A,

163   insert). The number of experimental mice was considered to be sufficient because the present

164   results represented statistically significant differences between the groups.

165   In the HCD group, the proportion of CL72:8 in relation to total CL level was found to be

166   strikingly decreased by 93% (P <0.0001) (Figure 1B). We also calculated total nascent CL level

167   (CLs other than CL72:8) by subtracting the CL72:8 level from the total CL level (Figure 1B).

168   The nascent CL level was increased in the HCD group compared with that in the NCD group (P

169   <0.01). Nascent CL was the predominant CL type in the HCD group (P <0.0001).

170   The fatty acyl profile of CL was different between the NCD and HCD groups (Figure

171   1C). The fatty acyl composition of CL revealed that FA18:2 was the predominant CL in the

172   NCD group, whereas FA18:2 was less predominant in the HCD group.

173

174   **3.2. Hepatic MLCL profile**

175   Nine types of MLCL were identified in the liver (Figure 2). MLCL54:6, derived from

176   CL72:8, was the most dominant type of CL in the NCD group. On the other hand, the level of

177   MLCL54:6 was found to be insignificant in the HCD group (P <0.01), whereas the levels of

178   other types were significantly higher in the HCD group than those in the NCD group. Total

179   MLCL level was calculated by adding all MLCL levels determined in this study and was 2.4-

180   fold higher in the HCD group than that in the NCD group (P <0.05) (Figure 2, insert).

181

182   **Gene expression analysis**

183   We analyzed the expression of genes involved in the CL remodeling process (Figure 3).

184   *Taz* expression was significantly downregulated in the HCD group compared with that in the

185   NCD group (P <0.05). *Lclat1* expression was also downregulated but it was not statistically

186   significant (P = 0.095). On the other hand, *Cls* expression was upregulated but it was not

187   statistically significant (P = 0.153). *Pnpla8* expression was similar between the two groups.

188

189   **Correlation between MLCL and nascent CL levels or *Taz* expression in the liver**

190   For determining the relationship between MLCL and nascent CL levels, we determined

191   the correlation coefficient (Figure 4). A strong positive correlation between the levels of nascent

192   CL (CLs other than mature CLs) and total MLCL was observed (r = 0.955, P <0.0001).

193   Similarly, we also determined the correlation coefficient of MLCL level and *Taz*

194   expression (Figure 4) and found a negative correlation between them (r = −0.593, P = 0.0883).

195

196 **Discussion**

197   To date, few studies have developed a mouse model for overeating-induced fatty liver

198 in which changes in MLCL and CL levels are induced only after 5 days of administering an

199 HCD. The results of our study were similar to a previous one in which downregulation of *Taz*

200 expression and reduction in mature CL level were observed in the isolated mitochondria of rat

201 fed with high amounts of sucrose for a long duration (24 weeks).[12] Thus, abnormal CL

202 metabolism could be hampered because of unhealthy and irregular ways of eating even for a

203 short period, thus indicating the effect of eating habits on human health.

204   We also reported that mitochondrial dysfunction could be caused by the low levels of

205 several proteins involved in mitochondrial biogenesis, such as peroxisome proliferator-activated

206 receptor gamma co-activator 1 alpha, mitochondrial thioredoxin, cardiolipin synthase,

207 peroxisome proliferator-activated receptor alpha,[11] indicating that reduction in CL level and

208 mitochondrial dysfunction could be directly related. CL is localized only in the mitochondrial

209 cristae, and is strongly associated with regulating mitochondrial function.[19] Furthermore, hepatic

210 CL level has been reported to be reduced in rats with non-alcoholic fatty liver,[8] which could

211 result in mitochondrial dysfunction. Similar to these reports, a reduction in CL level was

212 observed in the present mouse model of fatty liver (Figure 1A). Our mouse model could be

213 useful in elucidating the underlying mechanism of the interaction between hepatic lipid droplets

214 and the mitochondria in the future.

215   Figure 1 illustrates CL level modulation. Among the different types of CLs, CL72:8

216 possess the $(18:2)_4$ acyl chain and is considered to be a mature CL that plays a major functional

217 role in mammalian cells.[7,20-22] The $(18:2)_4$ acyl chain of CL is essential for its high affinity

218 binding to proteins on the mitochondrial inner membrane. Hepatic CL72:8 level was lower in

219 HCD group than in the NCD group.[23] In early type I and II diabetic mouse model, CL72:8 level

220 in cardiomyocytes was found to be reduced probably because of abnormal CL remodeling .[24]

221 Similarly, in the present study, hepatic CL72:8 level was markedly reduced, whereas MLCL

222 level was increased (Figure 1B), clearly indicating abnormal CL remodeling in our mouse

223 model.

224   CL remodeling enzymatically transfers the acyl group of phospholipids to MLCL,

225 mainly via Tafazzin, followed by the production of mature CL. This regular remodeling plays an

226 important role in maintaining mitochondrial function.[25] In another study, an increase in MLCL

227 level caused by abnormal CL remodeling was attributed to mitochondrial dysfunction.[26] MLCL

228 does not strongly interact with mitochondrial membrane proteins[27]   but causes an inadequate

229 production of electron transport chain-mediated ATP.[28] Interestingly, abnormality of CL

230 remodeling seems to be correlated with the development of fatty liver. Them5-knockout mice

231 developed not only fatty liver but also an increase in MLCL level.[29] *ALCAT-1* overexpression

232 increased hepatic lipid droplets and abnormal CL remodeling.[30] A recent study reported that

233 dietary fatty acids caused changes in hepatic mitochondrial CL levels and its fatty acid

234 composition in rats with non-alcoholic fatty liver disease developed by administering a fat- and

235 carbohydrate-rich diet for 8 weeks.[31] Since the phenotype associated with abnormal CL levels

236 could be easily established in our model that included normal mice, we believe that our model

237   could help in better understanding of the pathology and onset of disorders associated with CL

238   remodeling.

239   *Tafazzin* is a phospholipid-lysophospholipid transacylase that transfers an acyl group

240   from phospholipids to MLCL, and is encoded by *Taz*, which is a critical gene for CL remodeling.

241   A previous study reported pathological changes in mitochondrial membranes in myofibrils,

242   skeletal muscles, and myocardium in *Taz*-deficient mice.[32] Mutations in *Taz* have been

243   associated with Barth syndrome, which is characterized by mitochondrial deficiency.[33]

244   Therefore, *Taz* downregulation could critically impair the biosynthetic pathway of mature CL.

245   On the other hand, an adeno-associated virus-mediated *Taz* replacement therapy by intravenous

246   injection can strikingly improve mitochondrial structure and function, heart function and

247   systemic activity level in the *Taz*-knockout mouse, which has been used as a mouse model of

248   Barth syndrome.[34] Perhaps therapeutics targeting *Taz* could be able to maintain normal CL and

249   MLCL levels and restore mitochondrial function. Thus, our mouse model might be useful for

250   demonstrating the effects of food extract, compounds, and drugs against mitochondrial

251   dysfunction via *Taz* expression.

252   In our study, levels of CLs except for CL72:8and MLCL were found to be increased

253   simultaneously. We believe that our study is the first to demonstrate a strong correlation between

254   CL72:8 and MLCL levels (Figure 4A). Similar to the increase in MLCL, an increase in nascent

255   CL level may lead to a reduction in mitochondrial function.[35] Our data suggest that an increase in

256   the precursors of mature CL is expected to cause mitochondrial dysfunction associated with

257   abnormal CL metabolism in the liver. Moreover, MLCL levels were found to be negatively

258   correlated with *Taz* expression in the liver (Figure 4), which is in accordance with the

259   observation that *Taz* downregulation leads to increase in MLCL levels as reported in several

260   previous studies.[36-38]

261   However, there are several limitations of this study. First, the reason for the

262   downregulated expression of *Taz*, which was not observed for the other investigated genes, could

263   not be ascertained in our proposed model. Thus far, the identity of the factors that control *Taz*

264   expression upstream is unclear. Once they are identified, this issue may be resolved. Second, we

265   attributed abnormal CL remodeling to mitochondrial dysfunction as previously mentioned.[4, 5, 6, 12,

266   25, 26, 28, 35] Therefore, in our future studies, we will focus on hepatic mitochondrial function directly

267   to further elucidate the phenotype.

268   In conclusion, we found that HCD modulated fatty acyl compositions of CL and

269   MLCL through Tafazzin in the liver, which could lead to mitochondrial dysfunction. Our mouse

270   model of short-term overeating could be useful for elucidating the relationship between fatty

271   liver and mitochondrial dysfunction in the future.

272

273   **Author contributions**

274   T.S., H.S., H.S., H.C., and S.P.H. designed the study. T.S., Z.C. and S.P.H performed

275   lipidomics by LC/MS. T.H. performed the animal studies. T.S. and A.Y. performed hepatic gene

276   expression analysis using real-time PCR. T.S., Z.C., A.Y., and H.C. wrote this manuscript. All

277   authors have read and approved the final version of this manuscript.

278

287   **Conflicts of interest**

288   H. Satoh is employees of Nissei Bio Co., Ltd. H. Sekiguchi is employees of Life Science

289   Institute Co., Ltd.

290

291   **References**

292   1 Chicco AJ and Sparagna GC, Role of cardiolipin alterations in mitochondrial dysfunction and

293   disease. *Am J Physiol Cell Physiol* **292**:33–44 (2007).

294   2 Claypool SM and Koehler CM, The complexity of cardiolipin in health and disease. *Trends*

295   *Biochem Sci* **37**:32–41 (2012).

296   3 Pennington ER, Funaib K, Brown DA and Shaik SR, The role of cardiolipin concentration

297   and acyl chain composition on mitochondrial inner membrane molecular organization and

298   function. *Biochim Biophys Acta Mol Cell Biol Lipids* **1864**:1039–1052 (2019).

299   4 Xu Y, Sutachan JJ, Plesken H, Kelley RI and Schlame M, Characterization of lymphoblast

300   mitochondria from patients with Barth syndrome. *Lab Invest* **85**:823–830 (2005).

301   5 Song C, Zhang J, Qi S, Liu Z, Zhang X, Zheng Y *et al.*, Cardiolipin remodeling by ALCAT1

302   links mitochondrial dysfunction to Parkinson's diseases. *Aging Cell* **18**:e12941 (2019).

303   6 Ye C, Shen Z and Greenberg ML, Cardiolipin remodeling: a regulatory hub for modulating

304   cardiolipin metabolism and function. *J Bioenerg Biomembr* **48**:113–123 (2016).

305   7 Li J, Romestaing C, Han X, Li Y, Hao X, Wu Y *et al.*, Cardiolipin remodeling by ALCAT1

306   links oxidative stress and mitochondrial dysfunction to obesity. *Cell Metab* **12**:154–165

307   (2010).

308   8 Petrosillo G, Portincasa P, Grattagliano I, Casanova G, Matera M, Ruggiero FM *et al.*,

309   Mitochondrial dysfunction in rat with nonalcoholic fatty liver involvement of complex I,

310   reactive oxygen species and cardiolipin. *Biochim Biophys Acta Bioenerg* **1767**:1260–1267

311   (2007).

312   9 Pessayre D and Fromenty B, NASH: a mitochondrial disease. *J Hepatol* **42**:928– 940 (2005).

313   10   Labbe G, Pessayre D and Fromenty B, Drug-induced liver injury through mitochondrial

314   dysfunction: mechanisms and detection during preclinical safety studies. *Fundam Clin*

315   *Pharmacol* **22**:335–353 (2008).

316   11   Sakurai T, Hayasaka T, Sekiguchi H, Satoh H, Chen Z, Chiba H *et al.*, Dietary salmon milt

317   extracts attenuate hepatosteatosis and liver dysfunction in diet-induced fatty liver model. *J Sci*

318   *Food Agric* **99**:1675–1681 (2019).

319 12 Ruiz-Ramírez A, Barrios-Maya MA, López-Acosta O, Molina-Ortiz D and El-Hafidi M,

320 Cytochrome c release from rat liver mitochondria is compromised by increased saturated

321 cardiolipin species induced by sucrose feeding. *Am J Physiol Endocrinol Metab* **309**:E777–

322 786 (2015).

323 13 Delzenne NM, Hernaux NA and Taper HS, A new model of acute liver steatosis induced in

324 rats by fasting followed by refeeding a high carbohydrate-fat free diet. Biochemical and

325 morphological analysis. *J Hepatol* **26**:880–885 (1997).

326 14 Hara A and Radin NS, Lipid extraction of tissues with a low-toxicity solvent. *Anal Biochem*

327 **90**:420–426 (1978).

328 15 Chen Z, Wu Y, Ma YS, Kobayashi Y, Zhao YY, Miura Y *et al*., Profiling of cardiolipins and

329 their hydroperoxides in HepG2 cells by LC/MS. *Anal Bioanal Chem* **409**:5735–5745 (2017).

330 16 Sud M, Fahy E, Cotter D, Brown A, Dennis EA, Glass CK *et al*., LMSD: LIPID MAPS

331 structure database. *Nucleic Acids Res* **35**:D527–532 (2007).

332 17 Acaz-Fonseca E, Ortiz-Rodriguez A, Lopez-Rodriguez AB, Garcia-Segura LM and Astiz M,

333 Developmental sex differences in the metabolism of cardiolipin in mouse cerebral cortex

334 mitochondria. *Sci Rep* **7**:43878 (2017).

335 18 Chen CC, Lee TY, Kwok CF, Hsu YP, Shih KC, Lin YJ *et al*., Cannabinoid receptor type 1

336 mediates high-fat diet-induced insulin resistance by increasing forkhead box O1 activity in a

337 mouse model of obesity. *Int J Mol Med* **37**:743–754 (2016).

338 19 Paradies G, Paradies V, Ruggiero FM and Petrosillo G, Mitochondrial bioenergetics decay in

339 aging: beneficial effect of melatonin. *Cell Mol Life Sci* **74**:3897–3911 (2017).

340   20 Pennington ER, Funai K, Brown DA and Shaikh SR, The role of cardiolipin concentration

341   and acyl chain composition on mitochondrial inner membrane molecular organization and

342   function. *Biochim Biophys Acta Mol Cell Biol Lipids* **1864**:1039–1052 (2019).

343   21 Semba RD, Moaddel R, Zhang P, Ramsden CE and Ferrucci L, Tetra-linoleoyl cardiolipin

344   depletion plays a major role in the pathogenesis of sarcopenia. *Med Hypotheses* **127**:142–149

345   (2019).

346   22 Pennington ER, Fix A, Sullivan EM, Brown DA, Kennedy A and Shaikh SR, Distinct

347   membrane properties are differentially influenced by cardiolipin content and acyl chain

348   composition in biomimetic membranes. *Biochim Biophys Acta Biomembr* **1859**:257–267

349   (2017).

350   23 Jha P, McDevitt MT, Gupta R, Quiros PM, Williams EG, Gariani K *et al*., Systems analyses

351   reveal physiological roles and genetic regulators of liver lipid species. *Cell Syst* **6**:722–773

352   (2018).

353   24 Han X, Yang J, Yang K, Zhao Z, Abendschein DR and Gross RW, Alterations in myocardial

354   cardiolipin content and composition occur at the very earliest stages of diabetes: a shotgun

355   lipidomics study. *Biochemistry* **46**:6417-6428 (2007).

356   25 Acehan D, Xu Y, Stokes DL and Schlame M, Comparison of lymphoblast mitochondria from

357   normal subjects and patients with Barth syndrome using electron microscopic tomography.

358   *Lab Invest* **87**:40–48 (2007).

359   26 Duncan AL, Monolysocardiolipin (MLCL) interactions with mitochondrial membrane

360   proteins. *Biochem Soc Trans* **48**:993–1004 (2020).

361   27 Xu Y, Phoon CKL, Berno B, DSouza K, Hoedt E, Zhang G *et al.*, Loss of protein association

362   causes cardiolipin degradation in Barth syndrome. *Nat Chem Biol* **12**:641–647 (2016).

363   28 Hoffmann B, Stöckl A, Schlame M, Beyer K and Klingenberg M, The reconstituted

364   ADP/ATP carrier activity has an absolute requirement for cardiolipin as shown in cysteine

365   mutants. *J Biol Chem* **269**:1940–1944 (1994).

366   29 Zhuravleva E, Gut H, Hynx D, Marcellin D, Bleck CKE, Genoud C *et al.*, Acyl coenzyme A

367   thioesterase Them5/Acot15 is involved in cardiolipin remodeling and fatty liver development.

368   *Mol Cell Biol* **32**:2685–2697 (2012).

369   30 Wang L, Liu X, Nie J, Zhang J, Kimball SR, Zhang H *et al.*, ALCAT1 controls mitochondrial

370   etiology of fatty liver diseases, linking defective mitophagy to steatosis. *Hepatology* **61**:486–

371   496 (2015).

372   31 Aoun M, Fouret G, Michel F, Bonafos B, Ramos J, Cristol J *et al.*, Dietary fatty acids

373   modulate liver mitochondrial cardiolipin content and its fatty acid composition in rats with

374   nonalcoholic fatty liver disease. *J Bioenerg Biomembr* **44**:439–452 (2012).

375   32 Acehan D, Vaz F, Houtkooper RH, James J, Moore V, Tokunaga C *et al.*, Cardiac and skeletal

376   muscle defects in a mouse model of human Barth syndrome. *J Biol Chem* **286**:899–908

377   (2011).

378   33 Barth PG, Valianpour F, Bowen VM, Lam J, Duran M, Vaz FM *et al.*, X-linked cardioskeletal

379   myopathy and neutropenia (Barth syndrome): An update. *Am J Med Genet A* **126**:349–354

380   (2004).

381   34 Suzuki-Hatano S, Saha M, Rizzo SA, Witko RL, Gosiker BJ, Ramanathan M *et al.*, AAV-

382   mediated TAZ gene replacement restores mitochondrial and cardioskeletal function in Barth

383   syndrome. *Hum Gene Ther* **30**:139–154 (2019).

384   35 Monteiro JP, Pereira CV, Silva AM, Maciel E, Baldeiras I, Peixoto F *et al.*, Rapeseed oil-rich

385   diet alters hepatic mitochondrial membrane lipid composition and disrupts bioenergetics.

386   *Arch Toxicol* **87**:2151–2163 (2013).

387   36 Lou W, Reynolds CA, Li Y, Liu J, Hüttemann M, Schlame M *et al.*, Loss of tafazzin results in

388   decreased myoblast differentiation in C2C12 cells: A myoblast model of Barth syndrome and

389   cardiolipin deficiency. *Biochim Biophys Acta* **1863**:857–865 (2018).

390   37 Valianpour F, Mitsakos V, Schlemmer D, Towbin JA, Taylor JM, Ekert PG *et al.*,

391   Monolysocardiolipins accumulate in Barth syndrome but do not lead to enhanced apoptosis. *J*

392   *Lipid Res* **46**:1182–1195 (2005).

393   38 Richter-Dennerlein R, Korwitz A, Haag M, Tatsuta T, Dargazanli S, Baker M *et al.*,

394   DNAJC19, a mitochondrial cochaperone associated with cardiomyopathy, forms a complex

395   with prohibitins to regulate cardiolipin remodeling. *Cell Metab* **20**:158–171 (2014).

396

397

398

399

400   **Figure Legends**

401   **Figure 1. Analysis of cardiolipin level in liver tissues by LC/MS**

402 (A) Cardiolipin (CL) levels in the liver. The insert is a figure indicating total CL level,

403 which was calculated by adding the levels of all the CLs determined in this study. (B)

404 Comparison of the levels of CL72:8 and other CLs (nascent CLs) between the two groups. (C)

405 Summary of CL profile on the basis of each fatty acyl group. For all the data, each intensity was

406 normalized by mg of wet liver used for analysis (NCD, n = 3; HCD, n = 6). * P <0.05, ** P

407 <0.01, *** P <0.001, **** P <0.0001.

408

409 **Figure 2. Distribution of monolysocardiolipin in the liver samples**

410 MonolysoCL (MLCL) level in each group was simultaneously measured using

411 LC/MS. For all the data, each intensity was normalized by mg of wet liver used for analysis

412 (NCD, n = 3; HCD, n = 6). The insert is a figure illustrating total MLCL level, which was

413 calculated by adding the levels of all MLCL determined in this study. * P <0.05, ** P <0.01, ***

414 P <0.001 vs. the NCD group.

415

416 **Figure 3. Effect on *Taz* expression in the high carbohydrate diet-fed group**

417 *Taz* expression was analyzed by real-time PCR. The relative expression was

418 normalized to that of *Gapdh*. * P <0.05, **** P <0.001 vs. the HCD group.

419

420 **Figure 4. Correlation between total monolysocardiolipin and total nascent cardiolipin**

421 **levels and *Taz* expression**

422   (A) Pearson's correlation coefficient was calculated to determine the correlation

423   between total monolysoCL (MLCL) and total nascent cardiolipin (CL) levels. (B) Pearson's

424   correlation coefficient was calculated to determine the correlation between MLCL and *Taz*

425   expression.

426

427   **Figure 5. Hypothetical mechanism explaining mitochondrial dysfunction in the high**

428   **carbohydrate diet-fed group**

429   A high carbohydrate diet (HCD) fed for 5 days after 2 days of fasting lead to fatty liver

430   development in our mouse model. It also caused altered the levels of cardiolipin (CL) and mono-

431   lyso-CL (MLCL) in the liver. *Taz* downregulation could be involved in CL modulation. Thus, an

432   increase in nascent CL (CL other than CL72:8) and MLCL levels as well as a decrease in mature

433   CL (CL72:8) level via *Taz* downregulation may have resulted in mitochondrial dysfunction in

434   the HCD group even in the short term. PC, phosphatidylcholine; LysoPC, lyso-

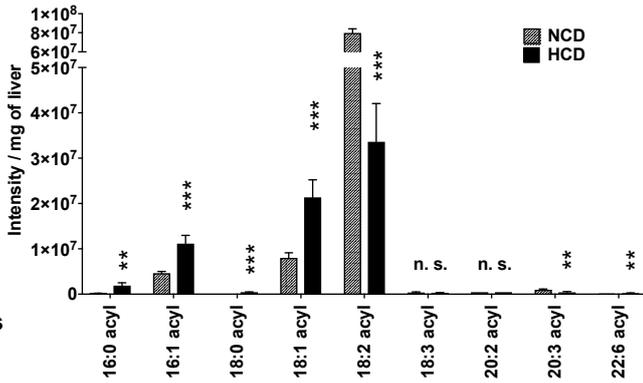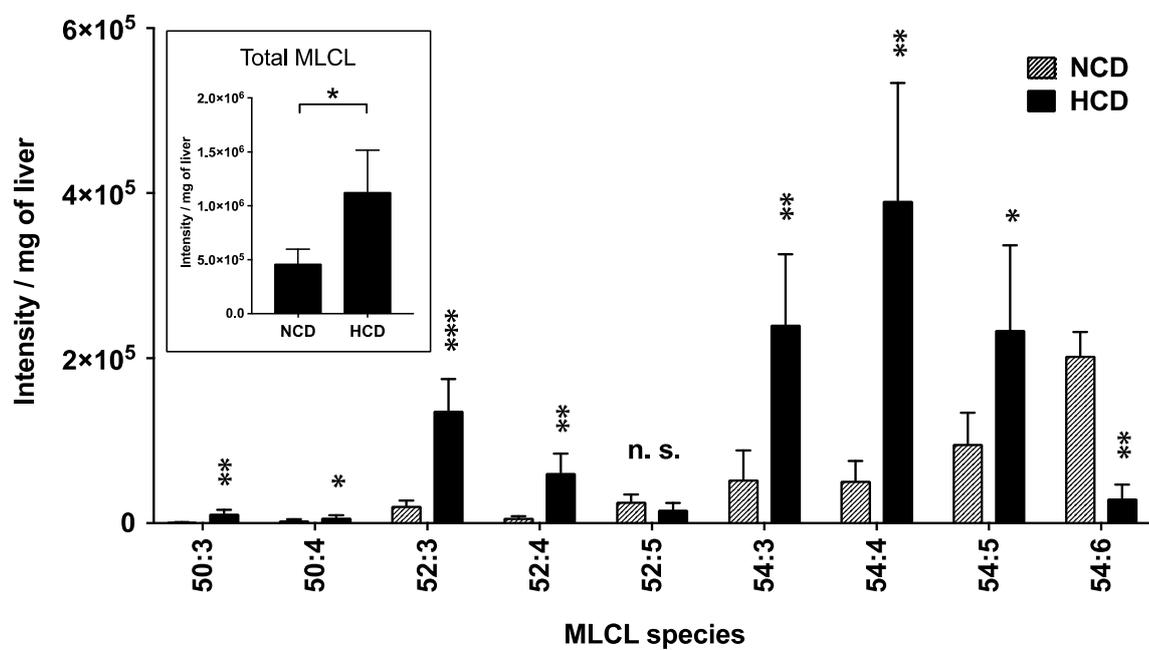435   phosphatidylcholine. PG, phosphatidylglycerol.

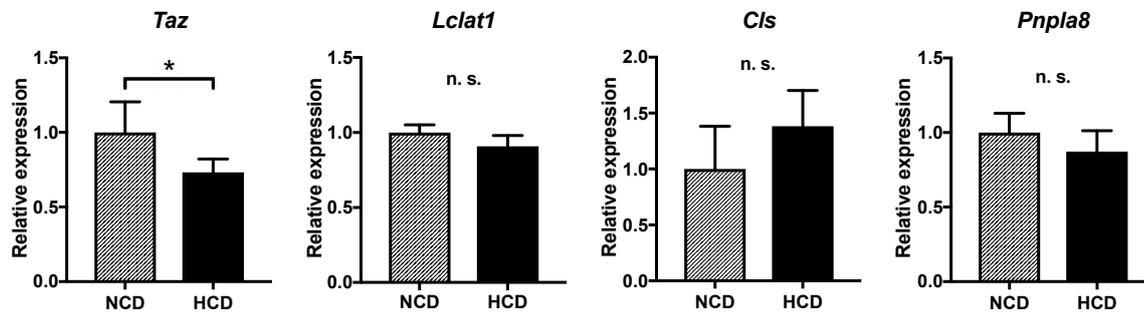**Figure 1.**
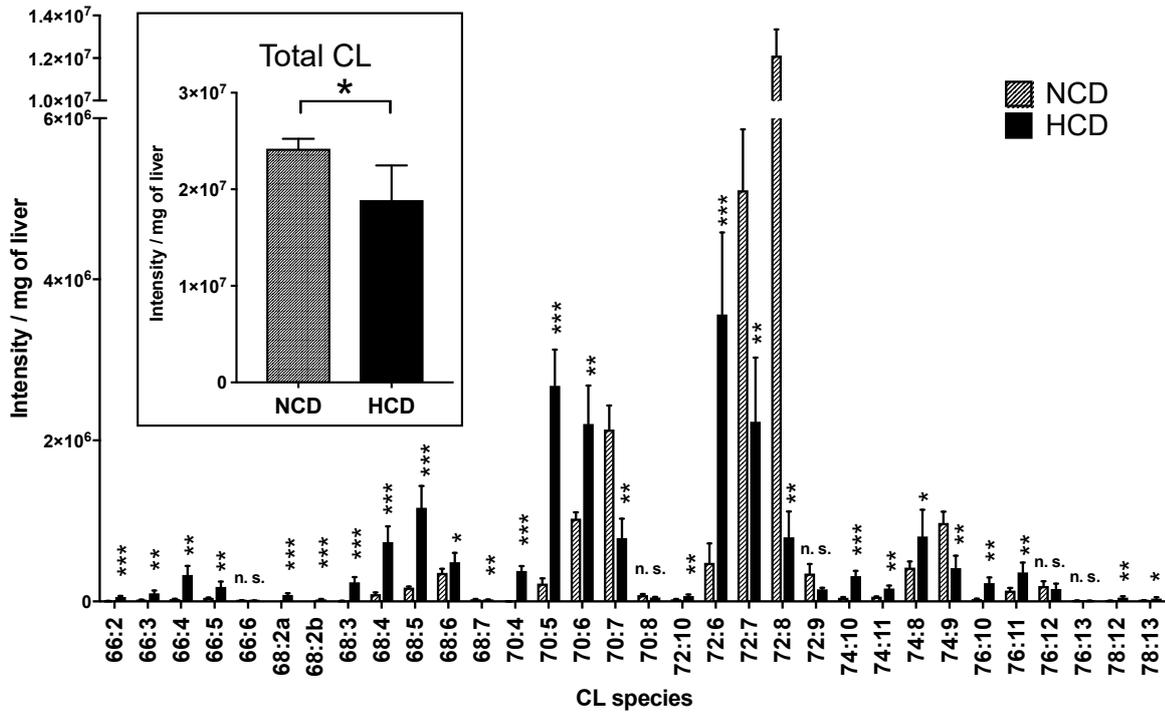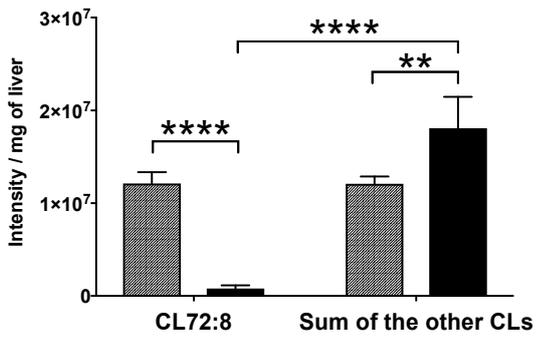
Figure 2.

Figure 3.

Figure 4.
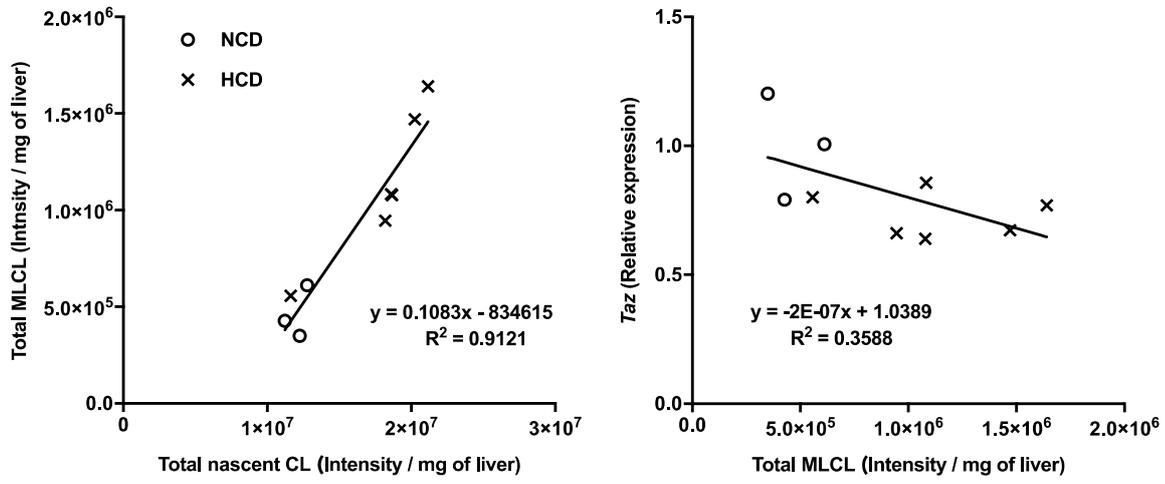
Figure 5.
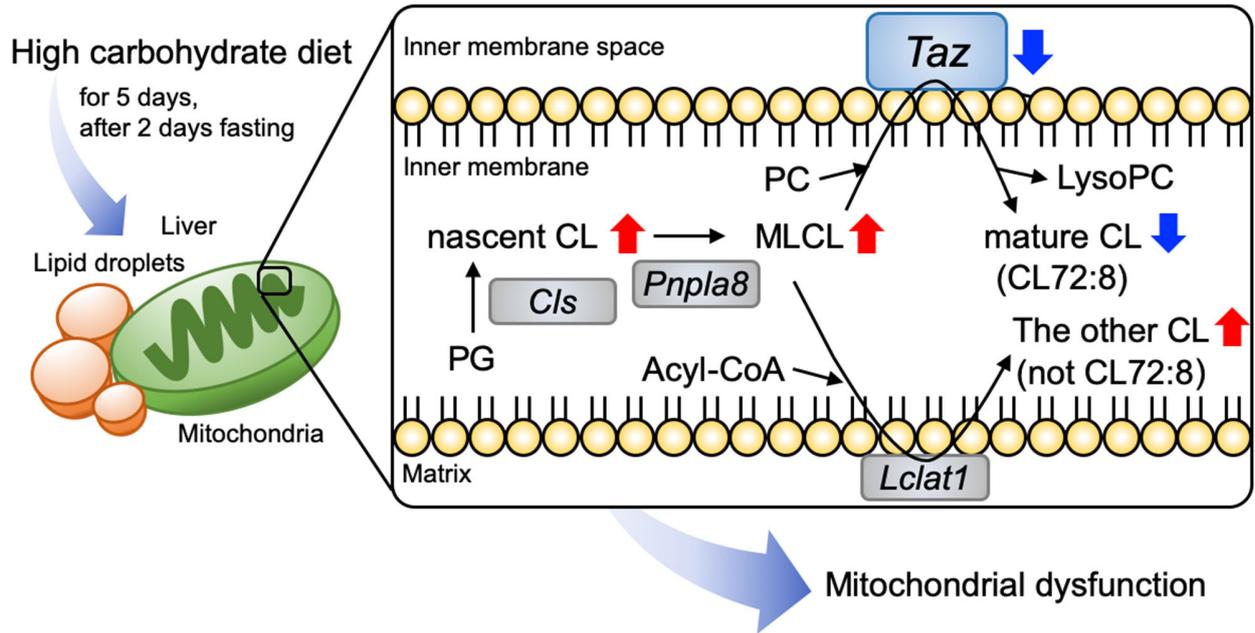
Supplemental Table1. Diet composition of HCD

	g kg^{-1}
Milk casein	160
Sucrose	380
Corn starch	380
Mineralmix	70
Vitamin mix	10

The special diet, high carbohydrate diet (HCD), was prepared from Hokudo Co. Ltd. (Sapporo, Japan).

Supplemental Table 2. Primer sequences for real-time PCR

Genes	Forward (5'-3')	Reverse (5'-3')	Ref.
Taz	CCTGAAGTTGATGCGTTGGA	GACACACAGGCACACATTTGC	17
Lclat1	GCATTTGTTAGTGGGAGAGTGCTA	GTAAGTTCCCAGCAGGATTAAAGTG	17
Cls	TGTAATGTTGATCGCTGCTGTGT	CCTAGCCGTGGCATAGCAA	17
Pnpla8	GGAATAGAAGTGAAGCACATTGCA	TAAGTCCCTTGGGAGCAGAAGT	17
Gapdh	TCACCACCATGGAGAAGGC	GCTAAGCAGTTGGTGGTGCA	18

Supplemental table 3. Identification of detected CL species

CL species	Calc. *m/z*	Tested *m/z*	Δppm	Fatty acyl composition
CL66:2	1375.9649	1375.9636	-0.94	N/A
CL66:3	1373.9493	1373.9523	2.18	N/A
CL66:4	1371.9336	1371.9348	0.87	16:1/18:1/16:1/16:1
CL66:5	1369.9180	1369.9188	0.58	16:1/18:2/16:1/16:1
CL66:6	1367.9023	1367.9020	-0.22	N/A
CL68:2a	1403.9962	1403.9960	-0.14	16:0/18:1/18:0/16:1
CL68:2b	1403.9962	1403.9977	1.07	16:0/18:1/18:1/16:0
CL68:3	1401.9806	1401.9830	1.71	16:1/18:1/18:1/16:0
CL68:4	1399.9649	1399.9672	1.64	16:1/18:1/18:1/16:1
CL68:5	1397.9493	1397.9509	1.14	16:1/18:2/18:1/16:1
CL68:6	1395.9336	1395.9338	0.14	16:1/18:2/18:2/16:1
CL68:7	1393.9180	1393.9186	0.43	N/A
CL70:4	1427.9962	1427.9976	0.98	16:1/18:1/18:2/18:0
CL70:5	1425.9806	1425.9814	0.56	16:1/18:1/18:2/18:1
CL70:6	1423.9649	1423.9648	-0.07	16:1/18:2/18:2/18:1
CL70:7	1421.9493	1421.9491	-0.14	16:1/18:2/18:2/18:2
CL70:8	1419.9336	1419.9309	-1.90	N/A
CL72:6	1451.9962	1451.9968	0.41	18:1/18:2/18:2/18:1
CL72:7	1449.9806	1449.9813	0.48	18:1/18:2/18:2/18:2
CL72:8	1447.9649	1447.9637	-0.83	18:2/18:2/18:2/18:2
CL72:9	1445.9493	1445.9442	-3.53	18:2/18:3/18:2/18:2
CL72:10	1443.9336	1443.9338	0.14	18:2/18:3/18:3/18:2
CL74:8	1475.9962	1475.9944	-1.22	18:2/20:2/18:2/18:2
CL74:9	1473.9806	1473.9790	-1.09	18:2/20:3/18:2/18:2
CL74:10	1471.9649	1471.9628	-1.43	N/A
CL74:11	1469.9493	1469.9478	-1.02	N/A
CL76:10	1499.9962	1499.9941	-1.40	18:1/22:6/18:2/18:1
CL76:11	1497.9806	1497.9777	-1.94	N/A
CL76:12	1495.9649	1495.9620	-1.94	N/A
CL76:13	1493.9493	1493.9495	0.13	N/A
CL78:12	1523.9962	1523.9906	-3.67	N/A
CL78:13	1521.9806	1521.9790	-1.05	N/A

N/A: Not available.